



Monitoring Urban Growth and Change Detection in Built-up Areas with High-Resolution Satellite Imageries

Received 23 May 2023; Revised 19 June 2023; Accepted 19 June 2023

Yousf A. Abas¹
Yasser G. Mostafa²
Mohamed A. BESHEER³
Mohamed F. A. Farrag⁴

Keywords

Urban growth, Change detection, image processing, information contents of satellite imageries.

Abstract

Recent developments in remote sensing provide very high-resolution imageries that are partially in competition with aerial images. This paper presents an evaluation of using IKONOS-2 and WorldView-2 satellite imageries for monitoring the growth of the built-up areas in the southern part of Assiut City between 2006 and 2016. In addition, a comparison between aerial orthoimage and satellite imagery was carried out. Also, a set of satellite imagery was downloaded from the Google Earth Pro application and used in this study to determine the rate of spatial growth in the southern part of Assiut City between 2011 and 2022.

The results of this study show that: Most map features can be detected and manually recognized from WorldView-2 imageries at a good level, while building detection was perfect. The applied change detection technique using IKONOS-2 imagery and WorldView-2 imagery shows that the growth of the built-up area in the south part of Assiut City between 2006 and 2016 is 783499.2 m², representing about 16.89 % of the total test area. Recent satellite imageries from open sources such as Google Earth were used successfully to determine the rate of spatial growth of the southern part of Assiut City in the period from 2011 to 2022. The spatial growth in this period was found to have increased dramatically, especially between 2014 and 2016. Remarkable negative changes were found in the agricultural lands due to the spatial growth of the built-up area in the south direction of Assiut City.

1. Introduction

The flow of people from rural to urban areas and the high population growth in addition to the high rate of economic development in Egypt require constructing of new human settlements which led to a major increase and change in the size of cities. Few of these new constructions were planned, while the majority were not and were illegally constructed. This can have a strong impact on the environment in many ways. Proper local and regional planning is only possible if it is based on up-to-date information about land cover, the distribution of natural resources, road networks, human

¹ Civil Eng. Dpt. Faculty of Engineering, Assiut University

² Civil Eng. Dpt. Faculty of Engineering, Sohag University

³ Civil Eng. Dpt. Faculty of Engineering, Assiut University

⁴ Civil Engineer M.Sc. Student

resources, and existing human settlements. The topographic maps that are the main data source for planners, are rapidly becoming out of date, and updating such maps is expensive and takes a long time. The objective of this study is to emphasize the role of high-resolution satellite imagery for monitoring urban growth and change detection in built-up areas. This study presents an evaluation of the information contents of the very high-resolution satellite imageries, where a comparison between the information contents of aerial orthoimage and WorldView-2 satellite imageries was carried out to emphasize the advantages and disadvantages of these data sources. Very high-resolution satellite imagery was used to detect changes in the built-up areas in the southern part of Assiut City between 2006 and 2016. In addition, a set of satellite imageries was downloaded from the Google Earth Pro application and used in this study to determine the rate of spatial growth in the southern part of Assiut City between 2011 and 2022.

2. Study Area and Used Data

2.1. Study area

This study was applied to the City of Assiut in Upper Egypt, Figure (1). Due to a limitation of the available data, the test area is limited to the southern part of the city. This part of Assiut City recently suffers from fast spatial growth in the built-up areas, some of the newly constructed buildings were planned, while the majority are illegally constructed. The geographical position of the test area (based on Helmer 1906 Ellipsoid) is $27^{\circ} 09' 16.5''$ N to $27^{\circ} 10' 38.9''$ N and $31^{\circ} 10' 25.6''$ E to $31^{\circ} 11' 59''$ E.

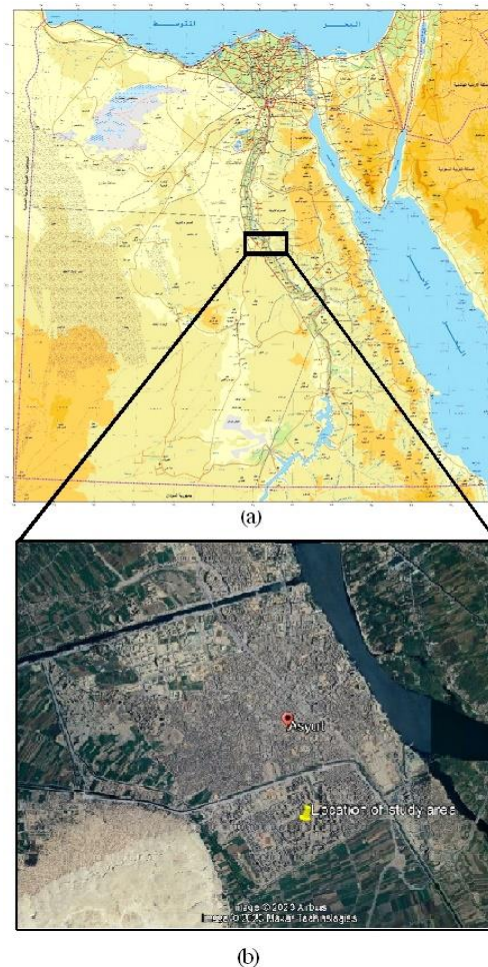


Figure (1) Location map of the study area. (a) Map of Egypt (b) Image of Assiut City from Google Earth

2.2 Used data.

The used data in this study are:

a- Two very high-resolution satellite imagery: IKONOS-2 satellite imagery that captured on 17th February 2006 (Plate-1) and WorldView-2 satellite imagery that captured on 4th March 2016 (Plate-2). The panchromatic bands and all multispectral bands of these imageries were used in this study and their characteristics are given in Table-1.

b- Aerial orthoimage of November 2015 (Plate-3).

ERDAS 2014 software was used to perform image processing and change detection techniques in this study.

Table-1. Characteristics of IKONOS-2 and WorldView-2 satellite imageries.

| Band | IKONOS-2 | | WorldView-2 | |
|--------------|-------------------------------|----------------|-------------------------------|---------------|
| | Wave length (μm) | Resolution (m) | Wave length (μm) | Resolution(m) |
| coastal blue | ---- | ---- | 400-450 | 1.84 |
| blue | 450-530 | 4 | 450-510 | 1.84 |
| green | 520-610 | 4 | 510-580 | 1.84 |
| yellow | ---- | ---- | 585-625 | 1.84 |
| red | 640-720 | 4 | 630-690 | 1.84 |
| red edge | ---- | ---- | 705-745 | 1.84 |
| near-IR1 | 760-860 | 4 | 770-895 | 1.84 |
| near-IR2 | ---- | ---- | 860-1040 | 1.84 |
| Pan | 450-900 | 1 | 450-800 | 0.46 |



Plate-1 IKONOS-2 (merged) satellite imagery of 2006

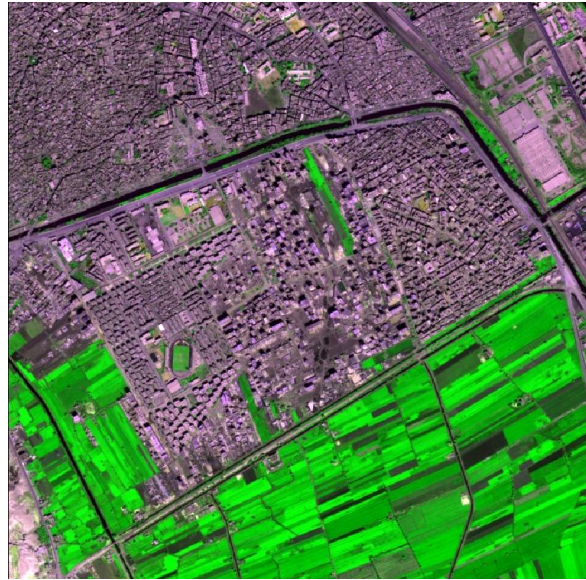


Plate-2 WorldView-2 (merged) satellite imagery of 2016



Plate-3 Orthoimage of 2015

3. Data Preprocessing

To prepare the images for an accurate comparison and change detection techniques, image registration and data fusion are required. Image registration is the process of fitting images to a known or common coordinate system. Accordingly, the tested satellite imageries and the aerial orthoimage need to be geo-referenced to a common coordinate system. The information contents or the feature declinability from satellite imageries can be increased as and when the spatial and spectral resolution of the satellite improves [Radhadevi et al, 2004]. The merge of low-resolution (multispectral) and high-resolution (panchromatic) satellite imageries improves the spatial resolution of the multispectral imagery and improves the overall performance of the remote sensing imageries for human visual perception and image processing task [Bing Li et al 2021]. A comprehensive review of image merging (or image fusion) techniques is given by [Bing Li et al 2021, Ghassemian 2016, and H.B. Mitchell, 2010]. The principal component analysis data fusion

technique is widely used to merge satellite imageries of different resolutions and was used in this study.

3.1. Image geo-referencing

Image geo-referencing is to geometrically register one image to another image that has been taken from different viewpoints at different times or by different sensors. In this study, the orthoimage is available in Egyptian Transverse Mercator (ETM) coordinate system. The IKONOS-2 imagery of 2006 and the WorldView-2 imagery of 2016 were geometrically registered to the aerial orthoimage using image-to-image registration that is available in ERDAS 2014 software. As a result of image geo-referencing the multispectral and panchromatic bands of IKONOS-2 imagery of 2006 and of the WorldView-2 imagery of 2016 were resampled to the same pixel size of the aerial orthoimage, which is 25 cm. To avoid changes in the digital numbers of the satellite imageries, the resampling was conducted using the nearest neighbour approach, while the geometric transformation was conducted using the second-order polynomial.

3.2. The principal component analysis data fusion technique

The aim of fusing high spatial resolution panchromatic and high spectral resolution multispectral images is to produce composite images that have the highest possible spatial information content and still preserving good spectral information quality. The Principal Component Analysis (PCA) technique transforms a multivariate inter-correlated data set into a new un-correlated data set. PCA synthesizes the original bands and creates new bands (the principal components) which pick up and reorganize most of the original band information. In general, the first principal component collects the information that is common to all the bands used as input data in the PCA (the spatial information) while the spectral information that is specific to each band is picked up in the other principal components. This makes PCA a suitable technique for merging multispectral and panchromatic imageries. In this case, all the bands of the original multispectral imagery constitute the input data. This transformation generates noncorrelated new bands and named the Principal Components (PC). The PC is substituted by the panchromatic image, whose histogram has previously been matched with that of the PC. In the final step, the inverse transformation is applied to the whole dataset formed by the modified panchromatic image and the PC2...PCn, obtaining that way the new fused bands with the spatial detail of panchromatic image incorporated into them [González et al, 2004]. The result of PCA data fusion technique of IKONOS-2 satellite imageries of 2006 is shown in Plate-1 and of WorldView-2 imageries of 2016 is shown in Plate-2.

4. Visual Comparison between WorldView-2 Satellite Imagery and Aerial Orthoimage

To evaluate the information contents of WorldView-2 satellite imagery a visual comparison between aerial orthoimage (that is approved for large-scale mapping), and satellite imagery was carried out. The National Imagery Interpretability Rating Scale (NIIRS) is a tool used to rate the quality of images captured by various imaging systems. The idea behind NIIRS is that as the interpretability of an image increases, imagery analysts can perform more complex interpretation tasks. The scale has 10 levels (0-9), each with its own set of interpretation tasks or criteria that

indicate the amount of information that can be extracted from an image at a specific level of interpretability [Gene Dial et al, 2003]. The graduated levels of NIIRS are illustrated in detail at: http://www.fas.org/irp/imint/niirs_c/index.html.

A classification/coding of topographic features for large-scale maps was published by National Digital Mapping Standards (NDMS), these objects are classified based on their level of detection and recognition [H. Sahin et al, 2004]. Detection is defined as: In imagery interpretation the discovering of the existence of an object, but without recognition of the object. Recognition is defined as: The ability to fix the identity of a feature or object in imagery within a group type [H. Sahin et al, 2004]. The classification of objects based on their level of detection and recognition is as follows: if an object can be detected and recognized easily and sharply, then it is assigned as "Perfect", if the level was lower than that, it is called "Good", if the object only detected or recognized, then it is put into the class of "Medium", if the level was very low, then it is "Poor" and if the object is not available in the imagery, it is categorized as "Not available" [Samadzadegan, 2004]. In this study, the detectability and recognizability of large-scale map features from the aerial orthoimage (which is approved for large-scale mapping) were conducted and the results are given in Table-2. These results were used as a reference to evaluate the information contents of WorldView-2 satellite imagery. Then the detectability and recognizability of the same features were conducted on the merged WorldView-2 satellite imagery and the results are given in Table-3.

4.1. Results of visual evaluation of the information contents of WorldView-2 satellite imagery.

From Table 2, it is very clear that aerial photography provides the most accurate data source for detecting and manual recognition of different features, making it the logical choice for large-scale mapping applications. The results of examining WorldView-2 imagery (Table 3) show that most map features can be detected and manually recognized at a good level, while building detection is perfect. Considering the advantages of satellite imagery, of covering large areas and being repeated very frequently, make it more suitable for periodical or annual change detection in some features such as built-up areas, agricultural land, road network, and water body for mapping and GIS applications.

Table-2 Summary of the aerial orthoimage information content

| SI No | Level 1 | Level 2 | Level 3 | Detectability | | | | | Manual Recognizability | | | | | |
|-------|------------------|--------------------|-----------------|---------------|------|--------|------|---------------|------------------------|------|--------|------|---------------|---|
| | | | | Perfect | Good | Medium | Poor | Not Available | Excellent | Good | Medium | Poor | Not Available | |
| 1 | Cultural Feature | Buildings | Residential | X | | | | | X | | | | | |
| | | | Commercial | X | | | | | X | | | | | |
| | | | Educational | X | | | | | X | | | | | |
| | | | Industrial | X | | | | | X | | | | | |
| | | | Religious | X | | | | | X | | | | | |
| | | | Historical | | | | | X | | | | | X | |
| | | Recreational | Health care | X | | | | | X | | | | | |
| | | | Park/Garden | X | | | | | X | | | | | |
| | | | Play Ground | X | | | | | X | | | | | |
| | | | Swimming Pool | | | | | X | | | | | X | |
| | | | Stadium | X | | | | | X | | | | | |
| | | | Beach | | | | | X | | | | | | X |
| | | Other | Tower | X | | | | | X | | | | | |
| | | | Mining area | | | | | X | | | | | | X |
| Fence | X | | | | | | X | | | | | | | |
| | | | | | | | | | | | | | | |
| 02 | Transport | Road class | Free way | | | | | X | | | | | X | |
| | | | District Road | X | | | | | X | | | | | |
| | | | Village Road | X | | | | | X | | | | | |
| | | | Street | X | | | | | X | | | | | |
| | | | Cart track | X | | | | | X | | | | | |
| | | | footpath | X | | | | | X | | | | | |
| | | Railway track | | | | | | X | | | | | | |
| | | Bridge | Bridge | X | | | | | X | | | | | |
| | | | Subway | | | | | X | | | | | | X |
| | | Transport Terminal | Railway station | | | | | X | | | | | | X |
| | | | Airport | | | | | X | | | | | | X |
| | | | Harbor/Port | | | | | X | | | | | | X |
| | | Others | Parking area | X | | | | X | | | | | | |
| | | | Traffic island | X | | | | X | | | | | | |
| 03 | Vegetation | Agricultural land | | X | | | | X | | | | | | |
| | | Tree | Single | | X | | | | X | | | | | |
| | | | Grove | | X | | | | X | | | | | |
| | | | Hedge | | X | | | | X | | | | | |
| 04 | Waste land | Wasteland | Barren | | X | | | | X | | | | | |
| | | | Rocky | | X | | | | X | | | | | |
| | | | Sandy | | X | | | | X | | | | | |
| | | | Sand dunes | | | | | X | | | | | X | |
| 05 | Hydrograph | Water body | River | X | | | | | X | | | | | |
| | | | Stream | X | | | | | X | | | | | |
| | | | Lake | | | | | X | | | | | X | |
| | | | Tank | | | | | X | | | | | X | |
| | | | Drain | X | | | | | X | | | | | |
| | | | Canal | X | | | | | X | | | | | |
| | | Structure | Aqueduct | X | | | | | X | | | | | |
| | | | Weir | X | | | | | X | | | | | |
| | | | Barrage | | | | | X | | | | | | X |
| | | | Dam | | | | | X | | | | | | X |
| | | Others | Island | | | | | X | | | | | | X |
| | | | Coral Reef | | | | | X | | | | | | X |

Table -3 Summary of the WorldView-2 satellite imagery information content.

| SI No | Level 1 | Level 2 | Level 3 | Detectability | | | | | Manual Recognizability | | | | | |
|-------|------------------|--------------------|-----------------|---------------|------|--------|------|---------------|------------------------|------|--------|------|---------------|---|
| | | | | Perfect | Good | Medium | Poor | Not Available | Excellent | Good | Medium | Poor | Not Available | |
| 1 | Cultural Feature | Buildings | Residential | X | | | | | | X | | | | |
| | | | Commercial | X | | | | | | X | | | | |
| | | | Educational | X | | | | | | X | | | | |
| | | | Industrial | | | | | X | | | | | | X |
| | | | Religious | | | X | | | | | X | | | |
| | | | Historical | | | | | X | | | | | | X |
| | | | Health care | | | X | | | | X | | | | |
| | | Recreational | Park/Garden | X | | | | | | X | | | | |
| | | | Play Ground | X | | | | | | X | | | | |
| | | | Swimming Pool | | | | | X | | | | | | X |
| | | | Stadium | X | | | | | | | X | | | |
| | | | Beach | | | | | X | | | | | | X |
| | | Other | Tower | | | X | | | | | | X | | |
| | | | Mining area | | | | | X | | | | | | X |
| Fence | | | X | | | | | | X | | | | | |
| 02 | Transport | Road class | Free way | | | | | X | | | | | X | |
| | | | District Road | X | | | | | X | | | | | |
| | | | Village Road | | X | | | | | | X | | | |
| | | | Street | | X | | | | | X | | | | |
| | | | Cart track | | X | | | | | | X | | | |
| | | | footpath | | | X | | | | | | X | | |
| | | Railway track | | X | | | | | | X | | | | |
| | | Bridge | Bridge | X | | | | | | X | | | | |
| | | | Subway | | | | | X | | | | | | X |
| | | Transport Terminal | Railway station | | | | | X | | | | | | X |
| | | | Airport | | | | | X | | | | | | X |
| | | | Harbor/Port | | | | | X | | | | | | X |
| | | Others | Parking area | | | X | | | | | | X | | |
| | | | Traffic island | | X | | | | | | X | | | |
| 03 | Vegetation | Agricultural land | | X | | | | | X | | | | | |
| | | Tree | Single | | X | | | | | X | | | | |
| | | | Grove | | X | | | | | X | | | | |
| | | | Hedge | | X | | | | | X | | | | |
| 04 | Waste land | Wasteland | Barren | | | X | | | | X | | | | |
| | | | Rocky | | X | | | | | X | | | | |
| | | | Sandy | | X | | | | | X | | | | |
| | | | Sand dunes | | | | | X | | | | | X | |
| 05 | Hydrograph | Water body | River | X | | | | | X | | | | | |
| | | | Stream | | | | | X | | | | | X | |
| | | | Lake | | | | | X | | | | | X | |
| | | | Tank | | | | | X | | | | | X | |
| | | | Drain | X | | | | | X | | | | | |
| | | | Canal | X | | | | | X | | | | | |
| | | Structure | Aqueduct | | | | X | | | | | | X | |
| | | | Weir | | | X | | | | | | X | | |
| | | | Barrage | | | | | X | | | | | X | |
| | | | Dam | | | | | X | | | | | X | |
| | | Others | Island | | | | | X | | | | | X | |
| | | | Coral Reef | | | | | X | | | | | X | |

5. Change Detection

The objective of applying change detection technique in this study is to determine the spatial growth in the southern part of Assiut City between 2006 and 2016. Image to image change detection technique was applied using two very high-resolution satellite imageries; IKONOS-2 imagery of 2006 and WorldView-2 imagery of 2016. Many researchers have used remotely sensed satellite data for change detection, and several approaches and techniques have been developed. Most change detection techniques fall into three general categories: image enhancement, multi-date data classification, and comparison of two independent land cover classifications [Mas, 1999]. Within these three approaches, there are several methods and techniques that can be applied. Details about these methods can be found in related publications such as [Lillesand and Kiefer 1994, James Anderson 2002, Farrag and Mostafa 2006]. The Post-Classification Comparison (PCC) for change detection is a pixel-by-pixel-based technique and is widely used with satellite imageries [Almutairi 2000 and Mamdouh 2016]. The post-classification comparison change detection technique is applied in this study to determine the spatial growth in the southern part of Assiut City between 2006 and 2016. The accuracy assessment of change detection follows the concept of error matrix [Story and Congalton, 1986], where overall accuracy and kappa coefficient were used for this purpose [Congalton, 1991 and Congalton and Green, 2008].

5.1. Post-classification comparison

Post-classification comparison technique, first perform multispectral classification on each source imagery, and then the resulting classifications are used to create a change matrix. The advantage of producing a change matrix is that it describes not only the number of changes but the type of changes that have occurred as well. The major weaknesses of these techniques are the time it takes to accurately classify imageries and the fact that any errors made in the classification are compounded in the detection of changes [Almutairi, A., 2000].

In this study, to perform the post-classification comparison, first supervised classification by maximum likelihood classification technique was carried out to classify each of IKONOS-2 multispectral imagery and WorldView-2 multispectral imagery into five main classes. The five classes are building, vegetation, bare soil, paved roads (asphalt), and water. Then the classified imageries were used as inputs to the processing program to create a change matrix. The changes between the two dates are summarized by five broad change categories: No Change (NC), Vegetation to Building (V-B), Vegetation to Soil (V-S), Soil to Vegetation (S-V), and Soil to Building (S-B). Plate-5 shows NC area in gray, V-B in red, V-S in Yellow, S-V in Green, and S-B in Brown. For accuracy assessment 574 samples were distributed randomly by the processing software and the error matrix is given in Table 4.

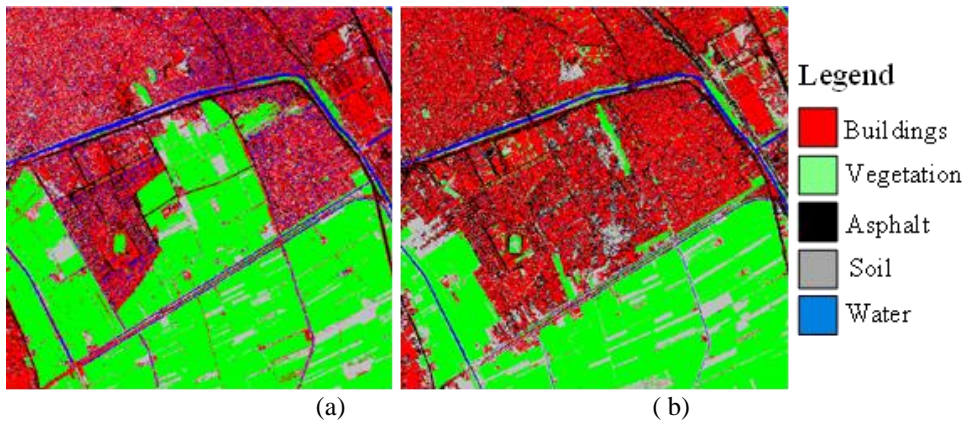


Plate-4 Classified IKONOS-2 and WorldView-2 imageries: a) Classified IKONOS-2 imagery of 2006 b) Classified WorldView-2 imagery of 2016

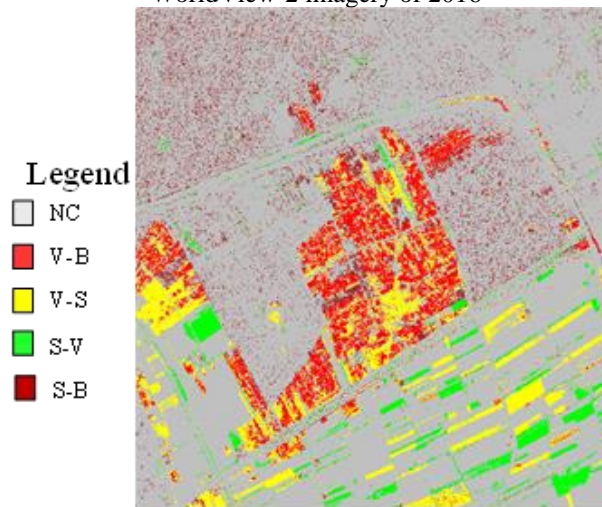


Plate-5: Post classification comparison of 2006 and 2016 satellite imageries

Table 4: Overall accuracy of change detection

| Classified Data | NC | V-B | V-S | S-V | S-B | Row Total | Users Accuracy | Producer's Accuracy |
|-----------------|-----|-----|-----|-----|-----|-----------|----------------|---------------------|
| NC | 370 | 9 | 0 | 7 | 4 | 390 | 94.87% | 97.63% |
| V-B | 2 | 46 | 4 | 0 | 0 | 52 | 88.46% | 69.70% |
| V-S | 4 | 8 | 46 | 0 | 0 | 58 | 79.31% | 92.00% |
| S-V | 2 | 0 | 0 | 20 | 6 | 28 | 71.43% | 64.52% |
| S-B | 1 | 3 | 0 | 4 | 38 | 46 | 82.61% | 79.17% |
| Column Total | 379 | 66 | 50 | 31 | 48 | 574 | | |

Overall accuracy = 90.59%

Over all Kappa = 82.29%

5.2. Results of image-to-image change detection technique.

Results of image-to-image change detection technique that applied to IKONOS-2 imagery of 2006 and WorldView-2 imagery of 2016 are summarized in Table-5.

Table-5 Quantitative results of changes

| Classified Data | Area (m ²) | % of total study area |
|-----------------|------------------------|-----------------------|
| NC | 3176802.56 | 68.49 |
| V-B | 417141.25 | 8.99 |
| V-S | 460106.88 | 9.92 |
| S-V | 217893.94 | 4.70 |
| S-B | 366357.94 | 7.90 |

The growth in built-up area is represented by: (V-B) plus (S-B). From Table-5 the growth in built up area represents about 16.89 % of the total test area.

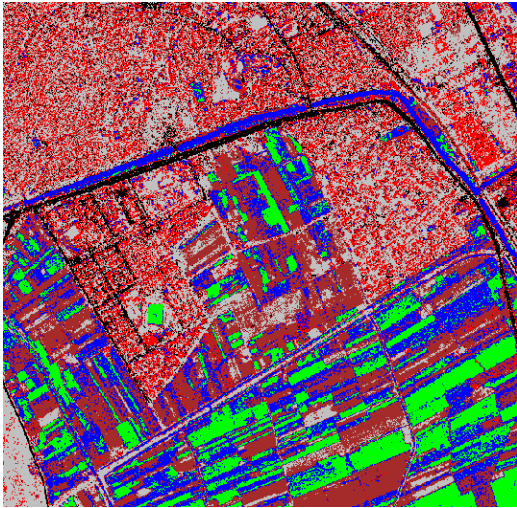
6. Rate of City Growth

Google Earth application is an open data source that can provide recent satellite imagery with high resolution. This study examines the use of imageries from this open data source for some useful applications such as the determination of the rate of spatial growth in cities. Set of multitemporal satellite imageries were downloaded from the Google Earth Pro application and used in this study to determine the rate of spatial growth in the south part of Assiut City between 2011 and 2022. Although the Google earth application can provide recent images with high spatial resolution, the downloading is restricted to three colours (RGB) with eight bits per pixel. This limits the spectral resolution of the downloaded imageries and can reduce the accuracy of image processing applications of such imageries. and field of applications of such imageries. The captured dates of the downloaded imageries are given in Table-6.

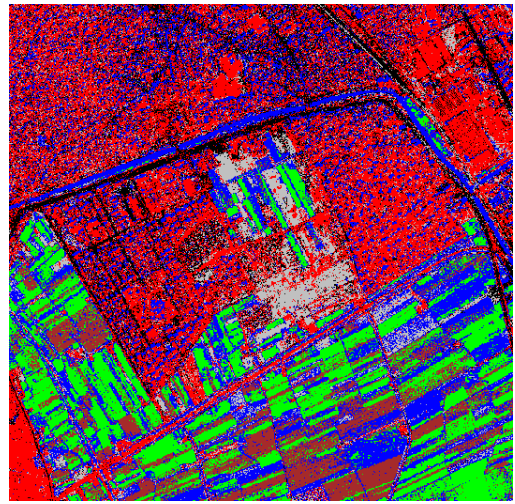
Table-6 Imageries used for determining the rate of growth.

| No | Date of imagery (Month/ Year) | No | Date of imagery (Month/ Year) |
|----|----------------------------------|----|----------------------------------|
| 1 | 7/ 2011 | 5 | 10/ 2018 |
| 2 | 2/ 2013 | 6 | 8/ 2020 |
| 3 | 11/ 2014 | 7 | 10/ 2022 |
| 4 | 10/ 2016 | | |

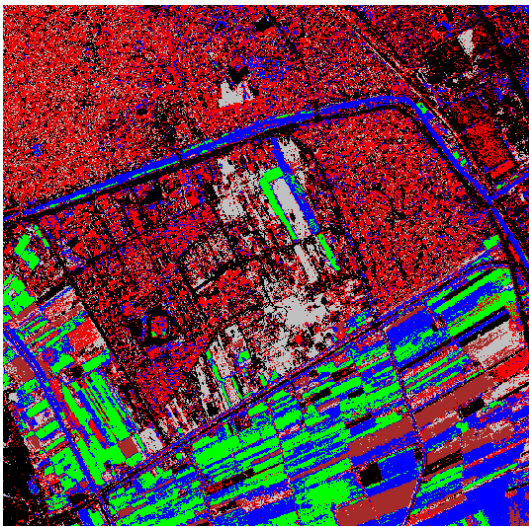
Post-classification comparison technique was used to detect multiannual change classes between this series of multitemporal imageries. To carry out the post-classification comparison, first, all imageries were geometrically registered to the available aerial orthoimage which is in Egyptian Transverse Mercator (ETM) coordinate system. As a result, all imageries were resampled to the same pixel size of the aerial orthoimage, which is 25 cm. The resampling was carried out using the nearest neighbour approach and the geometric transformation was applied using second-order polynomial transformation. Then supervised classification by maximum likelihood classification technique was carried out to classify each imagery to five main classes. The five classes are building, vegetation, bare soil, paved road (asphalt), and soil. Plate-6 shows the classified imageries.



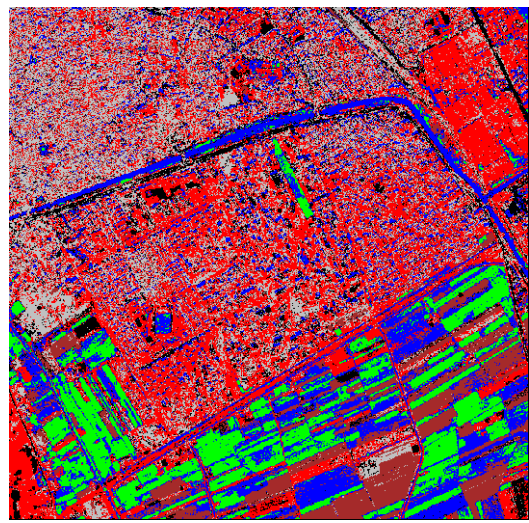
a. 2011 Classifies image



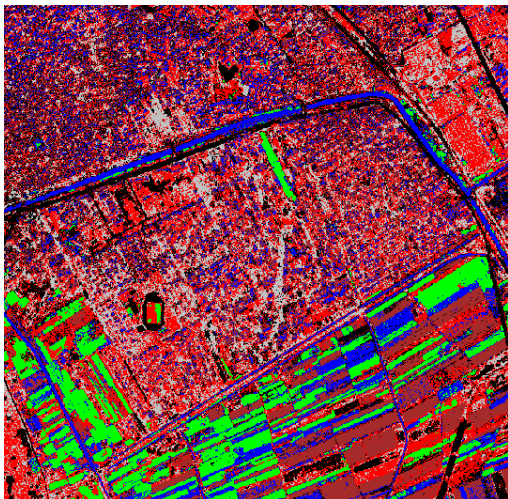
b. 2013 Classifies image



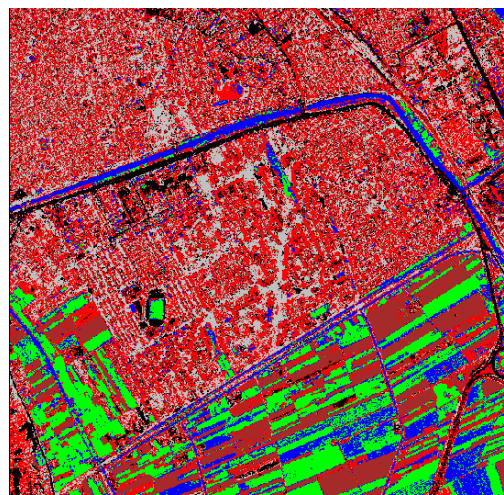
c. 2014 Classifies image



d. 2016 Classifies image



e. 2018 Classifies image



f. 2020 Classifies image

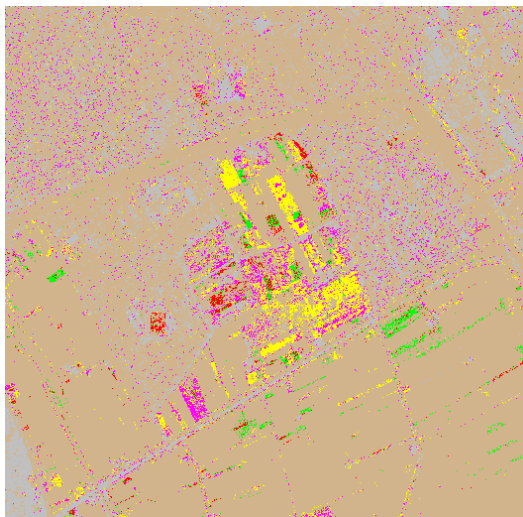


g- 2022 Classifies image

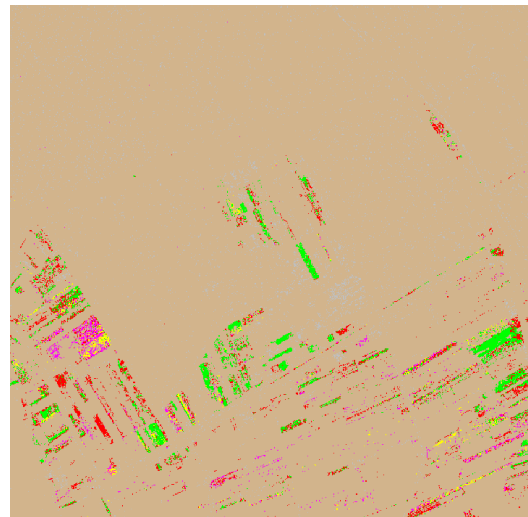
Legend: ■ Building ■ Vegetation ■ Bare Soil ■ Asphalt ■ Soil ■ Water

Plate-6 The classified imageries

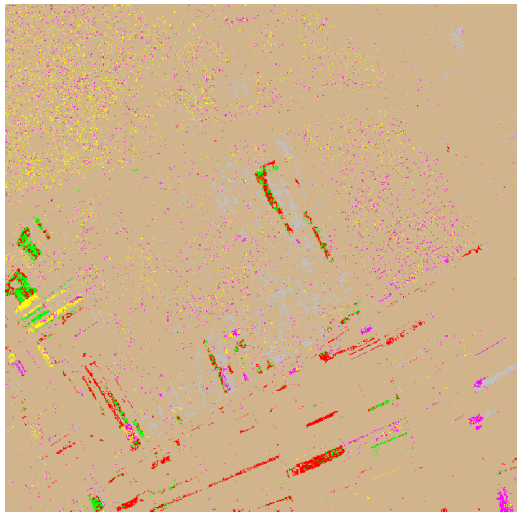
The classified imageries were used as inputs to the processing program to create a change matrix. The changes between every two successive dates are summarized by five broad change categories: Vegetation to Building (V-B), Vegetation to Soil (V-S), Bare soil to Soil (BS- S) Bare Soil to Building (BS-B), and Soil to Building (S-B). Plate-7 shows the results of the post-classification comparison technique. To carry out a quantitative analysis of the new built-up area three change categories were considered: Vegetation to Building (V-B), Bare Soil to Building (BS- B), and Soil to Building (S-B). Summary of the quantitative results are given in Table-7 and is represented graphically in Fig. 2.



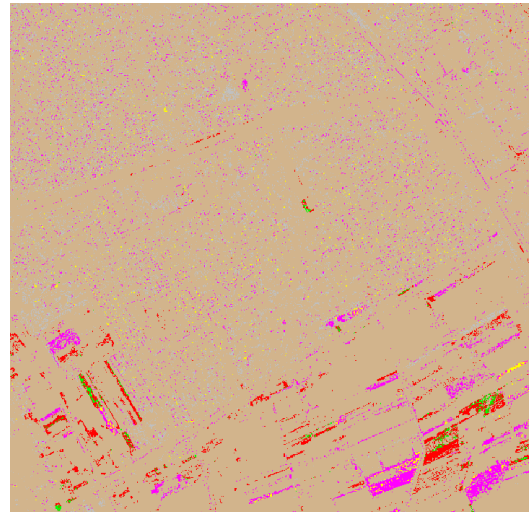
2011 & 2013 images



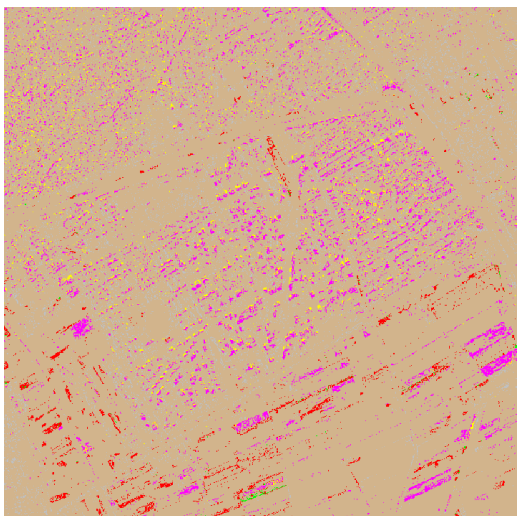
b 2013 & 2014 images



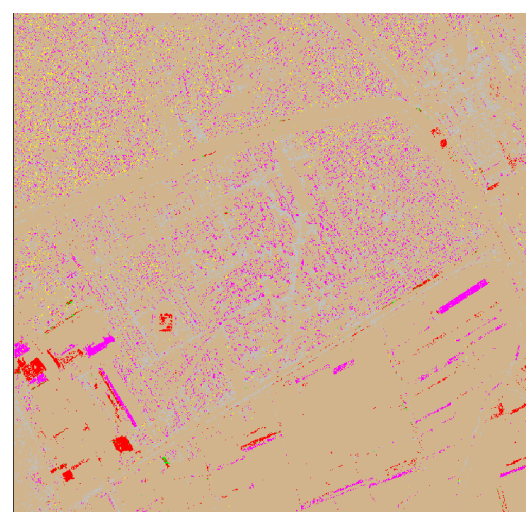
c 2014 & 2016 images



d 2016 & 2018 images



e 2018 & 2020 images



f 2020 & 2022 images



Plate-7 Results of post-classification comparison technique

6.1. Results of rate of City growth

New satellite imagery from open sources such as Google Earth is used successfully to determine the rate of the spatial growth of the southern part of Assiut City. The spatial growth of the southern part of Assiut City was found to be increased dramatically in the period from 2011 to 2022. Maximum spatial growth occurred between 2014 and 2016 and minimum spatial growth occurred between 2011 and 2013. Remarkable negative changes were found in the agricultural lands due to the spatial growth of the built-up area in the south direction of Assiut City

Table-7 Summary of post-classification comparison results

| No | Period (Date) | Period (month) | Area (m ²) of Change from Vegetation to Building | Area (m ²) of Change from Bare Soil to Building | Area (m ²) of Change from Soil to Building | New Built-up area (m ²) | New Built-up area (m ²) per month | Cumulative New Built-up area (m ²) |
|----|-------------------|----------------|--|---|--|-------------------------------------|---|--|
| 1 | From 2011 to 2013 | 19 | 15794.94 | 65418 | 43844.75 | 125057.69 | 6581.98 | 125057.69 |
| 2 | From 2013 to 2014 | 21 | 44681.69 | 69867.44 | 70470.88 | 185020.01 | 8810.48 | 310077.7 |
| 3 | From 2014 to 2016 | 23 | 50201.81 | 75353.75 | 300390.9 | 425946.46 | 18519.41 | 736024.16 |
| 4 | From 2016 to 2018 | 24 | 38278.81 | 42497.63 | 117882.2 | 198658.64 | 8277.44 | 934682.8 |
| 5 | From 2018 to 2020 | 22 | 16657.5 | 132471.3 | 137716.8 | 286845.6 | 13038.44 | 1221528.4 |
| 6 | From 2020 to 2022 | 26 | 102589.3 | 131503.9 | 86223.06 | 320316.26 | 12319.86 | 1541844.66 |

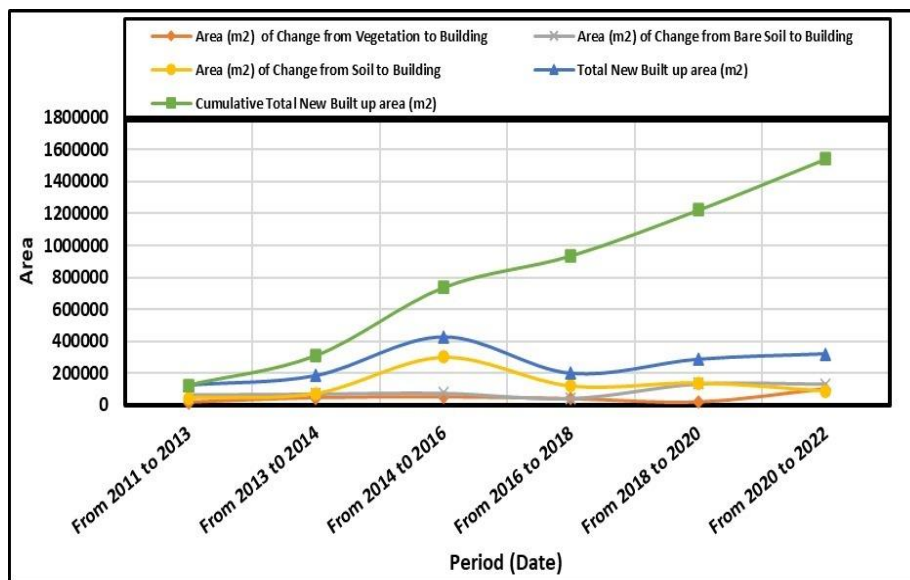


Figure (2) Results of post-classification comparison

7. Conclusion

The results of this study show that aerial photography provides the most accurate data source for detecting and manual recognition of different features, the pan-sharpened color imagery generated by merging 0.46-meter resolution panchromatic imagery with the 1.84-meter resolution multi-spectral bands of WorldView-2 satellite imagery provide exceptional depth in color and clarity of detailed for human visual perception and feature extraction. Most map features can be detected and manually recognized with a good level from the merged WorldView-2 imageries, while building detection is perfect. Considering the advantages of satellite imagery of covering a large area and being repeated very frequently, make it suitable for continuous (or periodical) detection of changes in some features such as built-up areas, agricultural land, road network, and water bodies, to be used for planning, updating of some map layers and GIS applications. The applied principal component comparison changes detection technique using IKONOS-2 imagery and WorldView-2 imagery shows that the growth of the built-up area in the south part of Assiut City between 2006 and 2016 is

783499.2 m² which represents about 16.89 % of the total test area. Remarkable negative changes were found, especially in the agricultural area due to the spatial growth of the built-up area in the south direction of Assiut City. Recent satellite imagery downloaded from open sources such as Google Earth were used successfully to determine the rate of spatial growth of the southern part of Assiut City in the period from 2011 to 2022. The spatial growth in this period was found to have increased dramatically, especially between 2014 and 2016 and the minimum spatial growth was between 2011 and 2013. Remarkable negative changes were found in the agricultural lands due to the spatial growth of the built-up area in the south direction of Assiut City.

References

1. Almutairi, A., 2000, Monitoring land-cover change detection in an arid urban environment: A comparison of change detection techniques. M.SC Thesis, college of Arts and Sciences, West Virginia University, USA.
2. Bing Li, Yong Xian, Daqiao Zhang, Juan Su, Xiaoxiang Hu, Weilin Guo (2021) Multi-Sensor Image Fusion: A Survey of the State of the Art
3. Journal of Computer and Communications, Vol.9 No.6, June 21, 2021
4. Congalton, R.G., 1991. A review of assessing the accuracy of classification of remotely sensed data, *Remote Sensing of Environment*, 37:35–46.
5. Congalton, R.G., and K. Green, 2008. *Assessing the Accuracy of Remotely Sensed Data: Principles and Practices*, Second edition, CRC Press, Taylor & Francis Group, Boca Raton, Florida).
6. Erdas imaging 9.1 field guides, 2008. volume one, version 9.1 (Erdas), Atlanta, USA.
7. Farrag A. Farrag, Yasser G. Mostafa, Nasser A. Mohamed (2020) Detecting Land Cover Changes Using VHR Satellite Images: A Comparative Study. *Journal of Engineering Sciences Assiut University, Faculty of Engineering*, Vol. 48 No. 2 March 2020 PP. 200–211
8. Farrag, A., and Mostafa, Y., 2006 "Comparison of Land Cover Change Detection Techniques with Satellite Images: Case Study in Assiut, Egypt" *Civil Engineering Research Magazine, Faculty of Engineering, Al-Azhar University, Volume 28, No. (3), pp. 983- 996.*
9. Gene Dial, Howard Bowen, Frank Gerlach, Jacek Grodecki, and Rick Oleszczuk,
10. Կօ՛՛. IKONOS satellite, imagery, and products. *Remote Sensing of Environment* 88, pp. 23–36
11. Ghassemian, H., 2016. "A review of remote sensing image fusion methods". *Information Fusion*, 32, pp.75-89.
12. González-Audícana, M., Saleta, J.L., Catalán, R.G. and García, R., 2004. "Fusion of multispectral and panchromatic images using improved IHS and PCA mergers based on wavelet decomposition". *IEEE Transactions on Geoscience and Remote sensing*, 42(6), pp.1291-1299.
13. Mitchell H.B., 2010. *Image Fusion Theories, Techniques and Applications*. Scientific Publishing Services Pvt. Ltd., Chennai, India, 2010 Springer-Verlag Berlin Heidelberg.
15. James Anderson., 2002, A comparison of four change detection techniques for two urban areas in the United States. Masters of Arts in geography, Eberly College of Arts and Sciences, West Virginia University USA.
16. Lillesand and Kiefer., 1994, *Remote sensing and image interpretation* (third edition). John wiley & Sons, Inc. New York. chichester. Brisbane, Toronto, Singapore.
17. Mas, J.F. 1999. Monitoring land-cover changes: a comparison of change detection techniques. *Int. J. Remote Sensing*. 20: 139-152.
18. Mamdouh M. El-Hattab 2016, Applying post classification change detection technique to monitor an Egyptian coastal zone (Abu Qir Bay). *The Egyptian Journal of Remote Sensing and Space Science*, Volume 19, Issue 1, June 2016, Pages 23-36
19. Radhadevi, P. V. V.Nagasubramanian, Archana Mahapatra, S.S.Solanki, Krishna
20. Sumanth and Geeta Varadan, 2004. Potential of High-Resolution Indian Remote Sensing Satellite Imagery for Large Scale Mapping.
21. http://www.isprs.org/proceedings/XXXVIII/1_4_7-W5/paper/Radhadevi-153.pdf . accessed June. 18, 2010.

22. Sahin, H.G. Buyuksalih, H. Akcin, H. Topan, S. Karakis, A. and Marangoz M.2004. Information Content Analysis of KVR-1000 Ortho-Image Based on the Available Topographic Maps in the GIS Environment. EARSEL Workshop on Remote Sensing for Developing Countries, Cairo, 2004.
23. Samadzadegan F, M Hahn, H Bagherzadeh & M Haeri, 2004. On the geometric accuracy and information content of IKONOS high resolution imagery for map revision. In: XX. Congress of ISPRS, (İstanbul, Turkey).
24. Satellite imaging corporation web site,2010.
25. <http://www.satimagingcorp.com/satellite-sensors/ikonos.html>
26. Satellite Imaging Corporation website, 2019. "Page Title: IKONOS Satellite Sensor" <https://www.satimagingcorp.com/satellite-sensors/ikonos/> Accessed on 14 July, 2019.
27. Story, M., and R.G. Congalton, 1986. Accuracy assessment: A user's perspective, Photogrammetric Engineering & Remote Sensing, 52(3):397–399.

مراقبة الزحف العمراني واستكشاف التغيرات على سطح الارض بواسطة صور الاقمار الصناعية عالية الدقة

الملخص

تتعرض بعض المدن في مصر لنمو مكاني عشوائي سريع عادة ما ينتج عنه آثار سلبية على البيئة. وبصفة عامة لا يمكن عمل تخطيط محلي أو إقليمي مناسب إلا بالاعتماد على معلومات دقيقة وحديثة. لذلك فإن جمع البيانات الحديثة ومراقبة النمو المكاني للمدن بشكل منتظم يعتبر من الضروريات الهامة لعمل تخطيط عمراني سليم وفعال. توفر التطورات الحديثة في الاستشعار عن بعد مرئيات فضائية عالية الدقة تتنافس جزئياً مع الصور الجوية ويمكن الاستفادة منها لهذه الأغراض. تم عمل مقارنة بين الصور الجوية (والمعتمدة عملياً في إنتاج الخرائط التفصيلية) ومرئيات الأقمار الصناعية للتأكيد على مزايا وعيوب كل من هذه المصادر في جمع البيانات اللازمة لإنتاج الخرائط المساحية وتحديث بعض معلوماتها. حيث تم تقييم استخدام صور الأقمار الصناعية IKONOS-2 و WorldView-2 لرصد نمو المناطق العمرانية بالتطبيق على الجزء الجنوبي من مدينة أسيوط بين عامي ٢٠٠٦ و ٢٠١٦. كما تم دراسة مدى الاستفادة من الصور الفضائية المجانية والحديثة عالية الدقة والمتاحة من خلال تطبيق Google Earth Pro لتحديد معدل النمو المكاني في الجزء الجنوبي من مدينة أسيوط بين عامي ٢٠١١ و ٢٠٢٢.

وقد أظهرت نتائج البحث أنه يمكن اكتشاف معظم عناصر الخرائط التفصيلية والتعرف عليها يدوياً من صور WorldView-2 بمستوى جيد، بينما كان اكتشاف المبنى مثاليًا. من أهم خصائص الاقمار الصناعية الحديثة انه يمكن الحصول على بياناتها بدقة وعلى فترات زمنية متقاربة مما يجعل مرئيات الاقمار الصناعية مناسبة لاكتشاف التغيرات في بعض التفاصيل مثل المناطق المبنية والأراضي الزراعية وشبكة الطرق والمساحات المائية. كما أظهرت تقنية اكتشاف التغيير باستخدام صور IKONOS-2 و صور WorldView-2 أن نمو المساحة المبنية في الجزء الجنوبي من مدينة أسيوط بين عامي ٢٠٠٦ و ٢٠١٦ هو ٧٨٣٤٩٩,٢ مترًا مربعًا، وهو ما يمثل حوالي ١٦,٨٩٪ من إجمالي مساحة منطقة الدراسة. كما أمكن استخدام مرئيات الاقمار الصناعية الحديثة وعالية الدقة من المصادر المجانية مثل Google Earth بنجاح لتحديد معدل النمو المكاني للجزء الجنوبي من مدينة أسيوط في الفترة من ٢٠١١ إلى ٢٠٢٢ حيث كان أعلى معدل في زيادة المناطق المبنية في الفترة بين ٢٠١٤ و ٢٠١٦. تم ملاحظة تغيرات سلبية ملحوظة في الأراضي الزراعية نتيجة النمو المكاني للمنطقة العمرانية في الاتجاه الجنوبي لمدينة أسيوط.